

SEGMENTED, PLEAT-FOLDED AND RIB-SUPPORTED THIN-SHELL COMPOSITE ANTENNA REFLECTOR

Juan M. Fernandez⁽¹⁾, Andrew F. Paddock⁽¹⁾, Kevin P. Roscoe⁽¹⁾, Kevin Demarco⁽²⁾

⁽¹⁾NASA Langley Research Center
Hampton, VA 23681, U.S.A.
Email:juan.m.fernandez@nasa.gov

⁽²⁾Analytical Mechanics Associates, Inc.
NASA LaRC, Hampton, VA 23681, U.S.A

Abstract

A new architecture scalable to sizes greater than 10 m for a deployable solid surface reflector antenna is presented. The design makes use of radially and circumferentially segmented thin-shell composite gores interconnected on the back side by a series of flexible shape memory composite elements. The reflector surface stows like an umbrella by creating serpentine-shaped pleats in the thin shell while being supported by a simple-hinged metering rib structure. A parametric study assessed how design features affect the deployed stiffness of the reflector and are used to identify a test matrix for manufacturing, foldability, and shape accuracy assessments. Various manufacturing tooling designs and dedicated folding fixtures were built to increase the fidelity and confidence of the test articles produced. An overview of the development effort is provided.

I. INTRODUCTION

Fixed solid surface reflector antennas are normally constructed up to a maximum diameter of 4 m due to the size of launch vehicle fairings. Given their high surface accuracy and low transmission losses, fixed solid surface reflector antennas can target higher radio frequencies than deployable mesh or membrane reflectors, which are more scalable in nature. To increase volumetric packaging efficiency, several efforts have targeted deployable solid surface reflectors. However, in general, those designs have been limited in size to less than 10 m in diameter due to high mass and mechanical complexity. The typical architecture is to have a central hub that is surrounded by a series of petals or gores supported on a deployable metering structure. The traditional approach is for these petals to be rigid, and thus such reflectors require a high degree of mechanical complexity in order to stow and deploy to the required accuracy, normally following a wrap-rib or radial and axial hinge approach. Researchers of advanced designs have investigated the use of deformable thin-shell composite reflective surfaces

made from low-thermal expansion, high-strain carbon fiber composite materials that allow the entire reflector to stow more efficiently by elastically deforming the material. In the United States, notable examples are the “Springback taco-shaped folded” reflectors developed by The Boeing Company[†] (Boeing) flown on several National Aeronautics and Space Administration (NASA) Tracking and Data Relay Satellites (TDRS) missions [1], the Multi-Arm Radial Composite (MARCO) reflector antenna concept developed at the U.S. Air Force Research Laboratory [2], the Flexible Precision Reflector (FPR) by Harris Corporation [3], and the Furlable Shape-Memory Reflectors (FSMR) by Composite Technology Development (CTD) [4-5]. The “Taco shell” design still shows low packaging efficiency and since it does not have a deep backbone structure, it does not scale up well. In the MARCO design the reflector is radially segmented into a series of deformable shell gores, each structurally independent and fixed to a radial arm that contains a rotating joint at the root location on the central hub, as well as at the radial arm mid-span to provide packing in two dimensions. The gore segments overlap the adjacent shells in a spiral pattern to package the reflector into a cylindrical shape requiring modest deformation of the gore elements. The FPR concept includes a non-segmented thin-shell composite reflector surface that is furled into a “serpentine”-pleated fashion, similar to the folds in a coffee filter or umbrella. This deformable structure is supported by a metering structure to provide deployment and stiffness. For very large versions, it was envisioned to divide the paraboloid into multiple circumferential rings that nest within one another during packaging. The FSMR design also does not have a segmented reflective surface and stows like an umbrella. Its key feature is that it uses shape memory composite circumferential stiffeners configured in a band that encloses at least a portion of the elastic reflector surface. These elements are used to constrain the stored strain energy of the deformable reflector surface to simplify the stowage and deployment of the reflector and reduce deployment dynamics and final shock loads. Scaling up

[†] Specific vendor and manufacturer names are explicitly mentioned only to accurately describe the analytical tools used. The use of vendor and manufacturer names does not

imply an endorsement by NASA nor does it imply that the specified equipment is the best available.

these types of architectures to larger than 5-m diameters require advancements in composite materials, structural design and computational tools, manufacturing tooling, and predictive cure-induced deformation software.

A new NASA feasibility effort was established in 2022 to explore high gain deployable reflector antenna designs scalable to more than 10-m diameter sizes that would need to achieve volumes and masses in line with state-of-the-art deployable mesh reflectors. An overview of the novel reflector concept is provided in this paper. The results of a parametric study that assesses how design parameters affect the deployed stiffness are presented first. The main design goal was to achieve a first deployed natural frequency of the reflector of 1 Hz at the 10-m scale while complying with mass and stowed volume requirements. A custom folding fixture that allows testing multiple gore designs with different paraboloid shape, subtended angle, and inner and outer radius was used to determine experimentally the best packing efficiency achievable in different reflector designs that were simulated. The results of the initial packaging tests were used to down select a final breadboard design for the concept demonstrator. The design and fabrication of a 1/6 sector of a 3-m diameter subscale breadboard model, representative of the entire full-scale system is presented. The final validation test campaign, followed by requirements compliance and concept feasibility assessment is expected in the last quarter of 2023.

II. DESIGN

A new segmented, solid surface antenna reflector concept constructed from a deformable thin-shell composite supported by single or dual-hinged radial arms that allows the structure to fold like an umbrella is presented [6]. A typical cylindrically stowed state for a 3-m reflector showing the inside diameter (ID), outside diameter (OD), and height (H) is shown in Fig. 1.

The new architecture combines several of the previously developed advantageous features: simple-hinged lightweight radial support arms; thin-shell composite reflective surfaces that are serpentine pleat-folded; and shape memory composites circumferential stiffeners. The key feature differentiating this architecture from previous concepts is that the reflective surface is segmented both radially and circumferentially and interconnected on the backside by discrete deformable composite substrate elements. Each thin-shell gore is also fixed along its centerline to the backbone deployable rib structure through a discrete number of flexible composite connectors. This segmentation and connections approach allows the reflective surface to stow efficiently into a rib-supported, umbrella-type configuration while providing adequate deployed stiffness and surface accuracy, and ease of manufacturing and assembly at large scales. The goal is to design an architecture that scales up by the design of the backbone structure rather than the

reflective surface. At very large scale, the use of the cantilevered radial ribs could be replaced by a more efficient truss structure. Finally, the use of a new shape memory composite substrate material with integrated heating and sensing capabilities reduces power requirements and the cost needed to scale up the system.

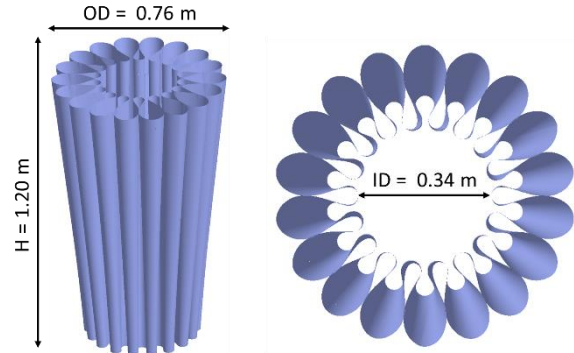


Fig. 1. Thin-shell umbrella-folded 3-m reflector: isometric view (left) and top view (right) showing typical ID, OD, and H values achievable with the technology proposed. The reflector stows by creating a serpentine pattern with 18 symmetric lobes/waves.

A. Parametric Study

A parametric study that assessed how design parameters affect the deployed stiffness of the reflector was first carried out using the finite element analysis software Abaqus. The main design goal was to achieve a first deployed natural frequency of the reflector of 1 Hz at the 10-m scale while complying with a total mass requirement for the antenna reflector of 50 kg and an enveloped stowed volume of 3 m³ (OD = 1 m x H = 3 m).

The finite element model (FEM) for the parametric analysis consisted of just the reflective surface with the flexible connecting features on the backside. The radial arms that form the backbone structure were neglected and thus ideal simplified boundary conditions (BC) were assumed at the discrete fixation points of the reflector to the arms. This approach enabled a faster design study that solely focused on the flexible composite elements. The goal was to maximize the deployed frequency of the paraboloid structure by trading different key features in the reflector. One of the FEM generated for the study is shown in Fig. 2. A mesh sensitivity study was first generated to define adequate mesh control parameters. Over 70 of these models were created using a parametric script in the pre-processor software PATRAN with a combination of these features. Jobs were then submitted to Abaqus for analysis and post-processing. The design parameters that were traded are as follows:

1. Reflector size or outside diameter: 3 m (breadboard demonstrator unit) vs 10 m (desired size).
2. Gore segment subtended angle (total number of gores): 30° (12 gores) vs 60° (6 gores).
3. Number of plies of the gore composite laminate: three or four plies at the 3-m scale, and four, five or six plies at the 10-m scale.

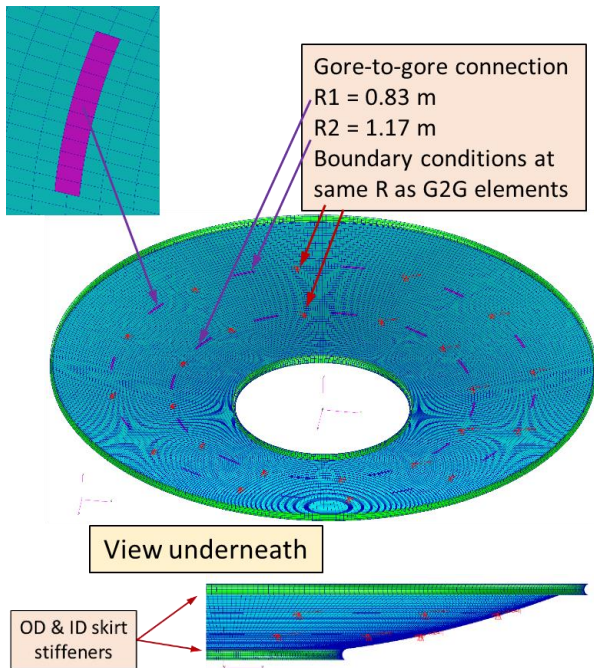


Fig. 2. Backside views of the FEM of a 3-m size, twelve gore (30°) reflector with two flat strip type gore-to-gore connections and two pad-up fixed points to the backbone per gore segment at the 0.83-m and 1.17-m radial stations (1/3rd and 2/3rd of the radial arc length of the parabola). The model has a four-ply laminate, continuous and concave inner and outer diameter skirt/rim stiffeners (shown in green), and a 0.5-m inner radius (central hole)

4. Number and degrees of freedom (DoF) of boundary conditions: one, two or three fixation points at each gore and constraint translation vs all-fixed DoF.
5. Outer rim/skirt shell design: concave vs convex.
6. Number of 20-cm long gore-to-gore (G2G) connections per gore.
7. Provide a curved tape-spring as the G2G connector or just a flat strip.
8. Circumferentially split outer skirt or continuous.
9. Align circumferentially the skirt joint locations to the BCs or have them staggered.
10. Provide pad-up boundary condition at the gore-to-backbone fixation points.
11. Radial location of gore-to-backbone connections.
12. Inner radius (IR) of the deployed gore, i.e. central hole size: 0.50 m (large) vs 0.375 m (medium) vs 0.25 m (small).
13. Split the 10-m reflector into two radially connected ~5-m reflectors or have it as a single unit.

Numerous conclusions were derived from the parametric study. The most relevant findings are:

- Increasing the number of G2G connections has the most influence on stiffness across the board. A 40% to 50% improvement in the lowest natural frequency at both size scales was achieved when

increasing the number of G2G elements from two to three. A total of three G2G elements was deemed as a good compromise between stiffness and fabrication complexity.

- Providing more gore-to-backbone supports stiffens the assembly; see Fig. 3. For a single BC per gore, locating it outboard was significantly better but still structurally insufficient. A 10% to 20% modest lowest frequency improvement was achieved from two to three BCs per gore. Therefore, two BCs is selected as a good compromise against complexity.
- Rotation fixity not a factor on stiffness. Translation BCs only is sufficient with at least one of the fixation points enabling radial translation during stowage and deployment.
- Moving the innerboard BCs from the 1/3rd to the 1/6th radial stations only influence significantly the 3-m size, twelve 30° gore reflector cases.
- Pad-up BCs do not increase global stiffness but effectively allow distribution of stresses over a wider area when a gravity load case is included in the analysis. Analysis for non-padded designs do not converge due to high localized stresses forming.
- The four-ply laminate performs better than the three-ply laminate at the 3-m scale, and is sufficient at the 10-m scale, improving mass over the five-and-six-ply designs.
- The number of total gores does not affect performance when the free-edge panel modes dominate. However, in general, the twelve-gore cases show a 10% to 20% stiffness increase over the six-gore cases at both reflector scales, as shown in Fig. 4.
- Providing G2G connectors as curved tape-springs (just like the skirts) rather than flat strip slightly improves the 10-m cases but not the 3-m cases.
- In general, the smaller inner radius degrade performance by lengthening the gore free edge that promotes lower panel modes, showing as much as 50% lower frequency modes than with a large central hole.
- Continuous skirts significantly stiffen the reflector. However, continuous outer rims cannot be fabricated to scale and likely will be post-bonded to the assembly. An effective design solution for the discontinuous convex skirt at the gore joint is found with two flat strips connecting the outboard and inboard edges of the neighbouring skirts. It provides a 40% to 60% lowest frequency increase with respect to cases with a complete disconnect, which promote gore torsional modes (windmill effect).
- Once gore free edge is stiffened, the skirt stiffness limits the frequency. Skirt stiffness is influenced by moving the gore-to-backbone boundary conditions closer to the skirts and the skirt size (bending moment of inertia). Whether the skirt is concave or convex does not affect stiffness, but for ease of gore

folding, the concave option is selected.

- The skirt joint locations are likely to be circumferentially staggered with the G2G joints when post-bonded. Staggering slightly improves reflector stiffness.
- Splitting the 10-m cases into an outer and inner disk and providing at least two BCs per gore and three G2G elements can provide deployed frequencies above 3 Hz.

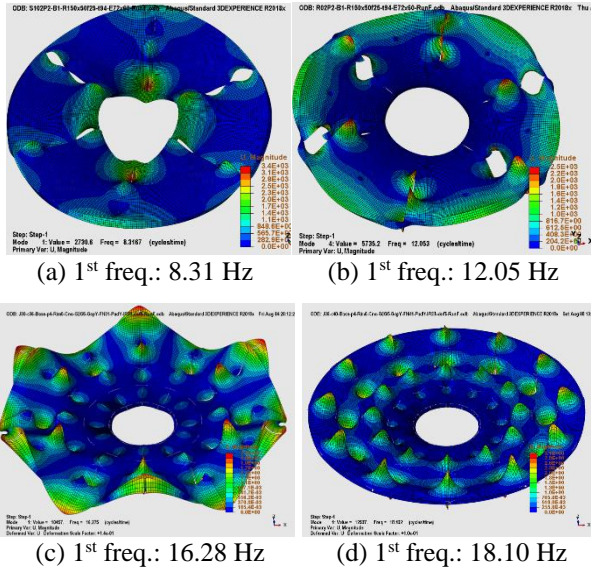


Fig. 3. Mid-gore fixity study for 3-m reflector. Six 60° gore reflector with IR = 0.5 m: (a) single BC located at gore mid-span; (b) two BCs at 1/3rd radial stations. Twelve 30° gore reflector with IR = 0.375 m: (c) two BCs at 1/3rd radial stations; (d) three BCs: one fixed at mid-span and two flexibles at 8% and 92% chord length.

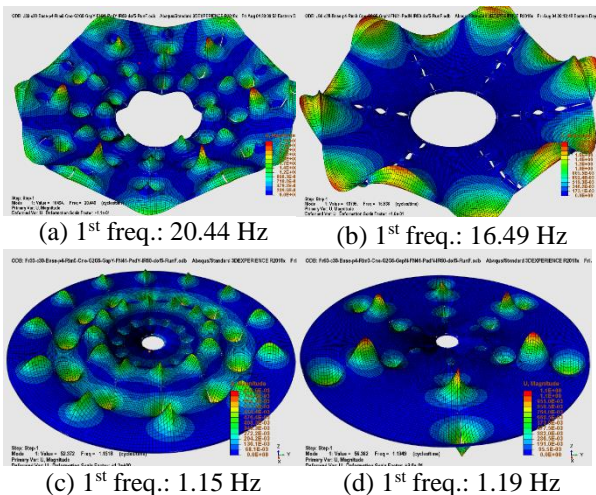


Fig. 4. Number of total gores study for a reflector with a 0.5-m inner radius, two BCs to the backbone, and three G2G connections: (a) 3-m case, twelve 30° gores; (b) 3-m case six 60° gores; (c) 10-m case, twelve 30° gores; (d) 10-m case, six 60° gores.

III. PROTOTYPE FABRICATION AND TESTING

A series of manufacturing development units (MDU) of the deformable reflector surface were produced to, first, generate confidence on both the ability to fabricate the thin-shell gores with built-in features and, second, to assess foldability of the paraboloid gores. The first MDU was a 60° gore test article of the inner 3-m disk of a 10-m outer diameter, D , parabolic reflector with a focus, F , of 7 m that yields a $F/D = 0.7$. The parabola equation is $Z = R^2 / 4F$, with Z being the height and R the radius. The parabola slope is $m = dZ/dR = R/2F$, and the normal is $m_N = -1/m$. The half-parabola reflector profile for three designs is shown in Fig. 5. The orange solid line represents the reflector profile of this first MDU, which was fabricated up to the manufacturing size limitation of $D = 3$ m represented by the black vertical solid line. The F/D ratio of 0.7 is the upper limit of the deeper parabolic reflector designs at the 10-m scale. The blue dashed line represents the bottom range of the shallower parabolic reflector designs at the 10-m scale ($F/D = 1.7$). Therefore, reflector designs between these curves are possible at the large scale, as the focal point would lay between 7 m and 17 m. The purple dotted line represents the second MDU fabricated, which had a much deeper paraboloid shape in line with an existing reflector design at the 3-m diameter scale.

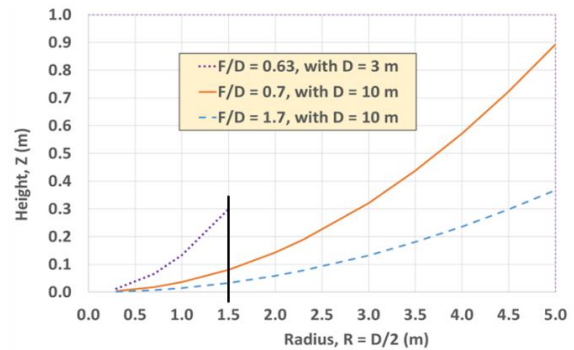


Fig. 5. Half-parabola of reflector profile. To generate the full paraboloid, each graph revolves around the vertical Z -axis. The solid vertical line represents the sub-scale model manufacturing size limit.

The mold for the first gore MDU was fabricated by assembling boards of Black Corintho 800[®] foam that have an operating temperature limit of 205°C. The blocks were bonded to create the desire tool volume using high temperature DUNAPOX Black AD 135 epoxy adhesive. The mold was then machined to shape and sealed with high temperature DUNAPOX Black SEA 125 epoxy sealer. This foam material has a coefficient of thermal expansion (CTE) at 180°C of 21 $\mu\text{m}/(\text{m}\cdot\text{K})$, which is $\sim 10\%$ lower than Aluminum and with 30% of the density. Therefore, it was chosen as an adequate low-cost tooling material for rapid prototyping. The tool produced and the associated surface error after fabrication are presented in Fig. 6.

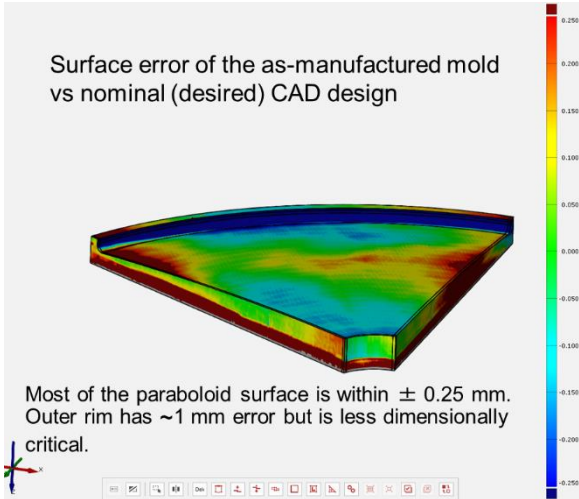
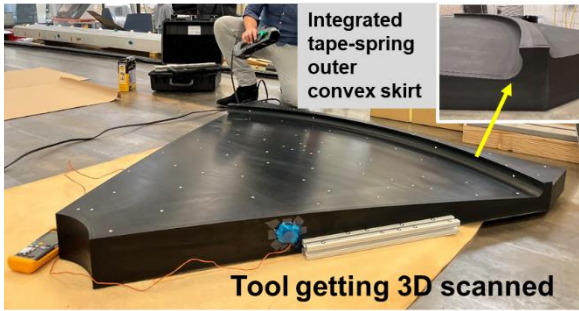


Fig. 6. Black Corintho[®] foam mold of the 60° gore getting scanned (top); and tool surface error contour plot with deviation range limits set at ± 0.25 mm.

Following a subsequent hot cure cycle to produce the first 60° gore, the three-dimensionally (3D) scanned deviation from the original design further increased from ± 0.25 mm after machining to about ± 0.8 mm due to small warpage of the foam material at 205°C, requiring re-machining of the tool to produce a second gore unit. It was determined that a lower upper limit of the gore cure cycle is necessary for continued use of this type of foam tool for precision applications.

Stowing of a segmented thin-shell reflector into a desired shape in a controlled manner requires the use of a dedicated folding fixture. A metal version with many mechanical joints was first envisioned for the final product. The mechanical concept that uses a series of linked metal rods that are interlaced with the thin-shell structure is shown in Fig. 7. The rods push this surface from the outside in and from the inside out to generate the constraints that form the serpentine shape of the stowed configuration. The rod links have ball rod ends for angular misalignment, enabling the external rods to follow equal rotations and provide global symmetry. To enable actuation of the external rods, which are hinged from a bottom ring, from the initial horizontal configuration in the reflector deployed state to the final vertical configuration in the stowed state, the external rods get moved by a series of linked middle rods hinged from a top ring that travel upwards. The final configuration has all rods vertically, generating a

cylindrical structure. The system behaves with similar folding kinematics to an umbrella.

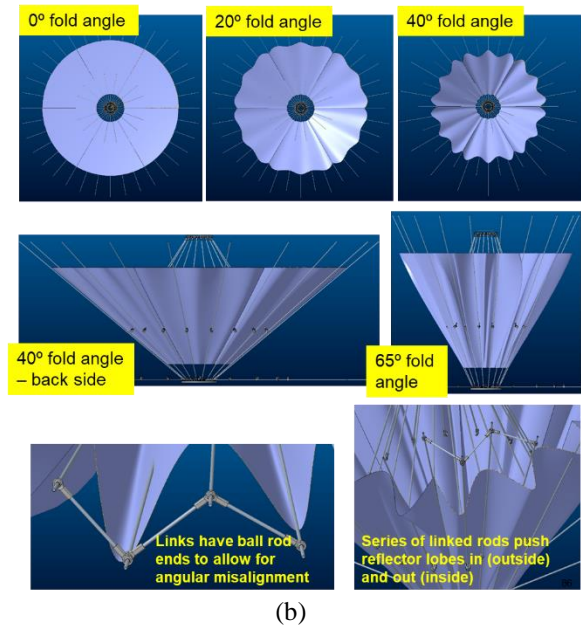
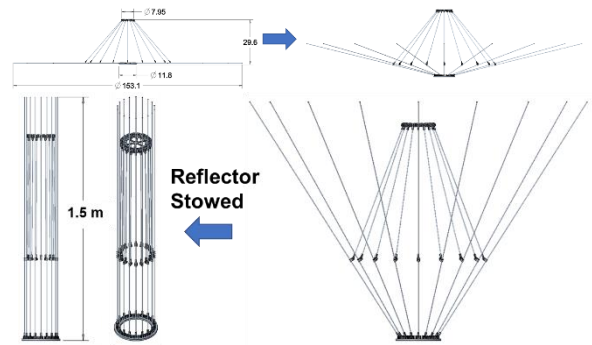


Fig. 7. (a) Mechanical steps of the envisioned ground support equipment (GSE) for folding the thin-shell reflector surface like an umbrella; (b) fixture coupled with a simulated reflector showing how the push rods enable folding a six-gore reflector.

For stowing the 60°-gore prototype MDU, a simplified version of this folding fixture was developed using wooden cylindrical solid rods with different diameter segments that followed the increasing desired diameters needed to effectively support the reflector surface along the radial directions: at the areas near the inner radius of the reflector, a 5.0-cm diameter rod segment was used; at the middle areas, a 6.3-cm rod segment was employed; and at the areas near the outer radius a 7.5-cm rod segment was used. The two free ends of the gore unit were initially taped to the outer two rods. A total of seven push rods initially created three waves or lobes in the shell as the three rods on the inside of the gore were held under gravity by the four rods on the outside that were initially raised a small amount, as shown in Fig. 8. The first motion consisted in closing the

thin shell like a fan by working in two parallel planes to the ground by moving the outer ends of the rods towards the centerline of the gore. The outside rods were mechanically hinged from the bottom of the fixture and were used to rotate the assembly 90° upwards into their vertical state, while the inner rods that were still held under gravity pushed the shell from the inside out. Once the gore was fully folded, the bottom ends of the inside rods were fixed to holes on the bottom of the fixture, positioning them at the necessary final angles. Ultimately, a clamp was used to fix the top of the outer rods against the top fixture, securing the assembly. The 60° gore was effectively folded without damage to a stowed height of 1.5 m and an outer radius of 0.45 m, following the pleated geometry generated by a prior finite element analysis.



Fig. 8. Folding steps of the first gore MDU using a wood fixture consisting of seven push rods (four on the outside and three on the inside of the gore) that generate three lobes in the shell. The outside rods are hinged at the bottom to enable 90° upwards rotation.

The second MDU design was a 30° gore of a 3-m outer diameter parabolic reflector with $F = 1.89$ m, which yields a $F/D = 0.63$. The parabola equation is $Z = R^2 / 4F$ and corresponds to the purple dotted curve shown in Fig. 5. A new foam mold was manufactured for this much deeper paraboloid by remachining to the desired shape an existing, narrow, high temperature FR-4718 foam tool and sealing the tool surface with Loctite EA 9394/C-2 epoxy adhesive. This foam material has a high CTE of $47 \mu\text{m}/(\text{m}\cdot\text{K})$, which is double of Aluminum, and thus cure-induced deformation of the final part was expected. The prior shallow gores constructed were very sensitive to gravity effects that tended to flatten them and thus obtaining a measurable accurate shape without the backing structure support was challenging. The objective of adopting this deeper paraboloid gore was to work with a test article that kept most of its curvature under gravity. The paraboloid followed a prior reflector design at the 3-m scale.

The goal of the gore test articles fabricated was to study different feasible reflector designs to assess the best packaging efficiency achievable. These designs used a combination of gore angle (30°, 22.5°, 18° and 15°) and deployed inner radius (IR from 0.25 m to 0.50 m) that were stowed to various preselected folded gore IRs using 3.8-cm and/or 5.0-cm diameter rods. A

new folding fixture was produced to effectively fold the gores into a single lobe/wave configuration. The objective was to assess folding in an equivalent configuration with a proportionally larger number of lobes/waves. For example, the 15° gore cases assessed folding of a 30° gore into two lobes, a 45° gore into three lobes, or a 60° gore into four lobes. The sawhorse-like folding fixture is shown in Fig. 9 stowing the test article from Case #2: 30° gore with a deployed IR = 0.3 m and stowed to a folded IR = 0.13 m using the 3.8-cm rods. The angle between the A-frame legs of the fixture matches the gore angle. The fixture helps progressively folds the gore by moving inboard one rod horizontally while the other rod remains fixed at the desired folded IR and clocked by half of the gore angle about the axis of the rod. The gore naturally sags under gravity providing a realistic folded shape.

The folding strains in the deployed gore IR region increased from Test Cases #1-8 as the gore angle reduced. The geometric dimensions of the key features of the deployed and stowed gore configurations used on the eight test articles are presented in Table 1. All eight cases tested were successful. No visual damage was observed on the gores during the folding process. Therefore, multiple reflector designs are possible in terms of number of gores, central hole sizes, and packaged configurations.

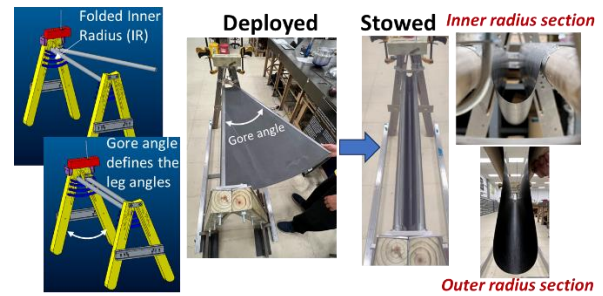


Fig. 9 Sawhorse folding fixture stowing a 30°-gore (Case #2).

Table 1. Geometric parameters for the single-wave folded test cases.

Case # / Feature dimension	1	2	3	4	5	6	7	8
Gore subtended angle (°)	30	30	22.5	22.5	18	18	15	15
Deployed Gore IR (m)	0.30	0.30	0.30	0.40	0.40	0.50	0.50	0.50
Folded Gore IR (m)	0.17	0.13	0.17	0.23	0.23	0.30	0.30	0.23
Rod diameter (cm)	5.0	3.8	3.8	5.0	3.8	5.0	3.8	3.8

IV. FINAL FABRICATION AND TESTING

The final breadboard test articles to be produced in this feasibility project are getting manufactured using a high-performance carbon foam mold. CFOAM 30® has a CTE of $5 \mu\text{m}/(\text{m}\cdot\text{K})$ at temperatures above 200°C, which is of the same order of magnitude of carbon fiber reinforced plastic (CFRP) laminates, incurring in

minimal cure-induced deformation from tool and part thermal expansion mismatch. The machined foam mold was sealed with ES-215 epoxy resin mixed with IHG hardener that is used in high-temperature composite tooling. Dedicated molds for the outer and inner tape-spring rims were also manufactured out of CFOAM 30[®]. The gores have a four-ply laminate construction from a 60 g/m² fiber areal weight, thin-ply plain weave (PW) M30S carbon fiber/PMT-F7 toughened epoxy material. The rims use the same thin-ply M30S PW fabric but infused with a new epoxy-based shape-memory-polymer resin system developed at NASA Langley Research Center (LaRC) for this project [7]. Embedded heaters in the laminate actuate the shape memory composite (SMC) skirts to finalize the gore deployment in a quasi-static manner.

Two full-scale gore test articles of the 3-m diameter reflector of increasing complexity and resemblance to the final design will be fabricated and tested:

- One 60° gore with a cutout IR = 0.3 m to be stowed as a three-lobe configuration with a central 3.8-cm square tube serving as the CFRP backbone arm connected by a fixed and a flexible BC along the gore centerline at the 1/3rd and 2/3rd radial stations. The arm will be tucked into the central inside radius lobe when packaged, as shown in Fig. 10 (a). Two smaller GSE rods will support the gore free edges. The gore will be stowed using 5-cm diameter rods in a configuration similar to Case #1 from Table 1, but at a folded IR = 0.17 m and OR = 0.39 m.

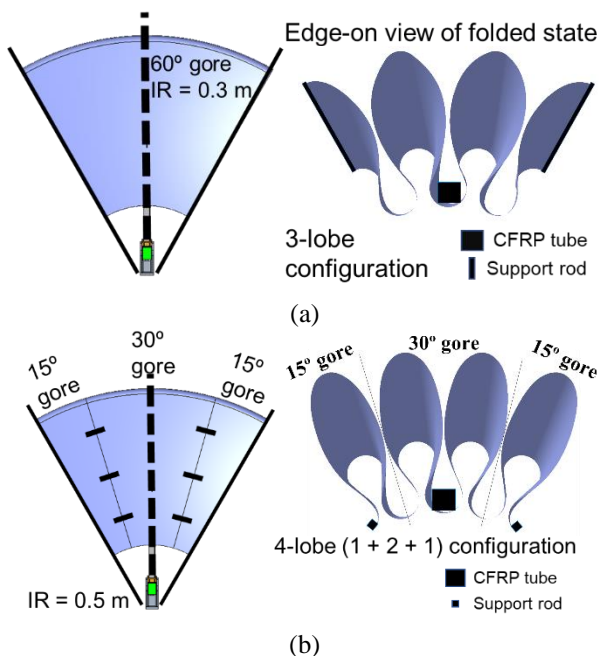


Fig. 10. Test articles to be produced for the final test campaign: (a) One 60° gore with a cutout IR = 0.3 m to be packaged as a three-lobe configuration; (b) One central 30° gore with two 15° gores attached with a cutout IR = 0.5 m to be packaged as a four-lobe assembled configuration.

- One central 30° gore with two 15° side gores attached to it via the inner and outer rims and three flat-strip G2G connectors at the 8%, 50%, and 92% arc-length radial stations. All the gores with a cutout IR = 0.5 m. The assembly will be folded using 3.8-cm rods into a four-lobe configuration with two lobes on the 30° gore and one lobe on each 15° gore resembling Case #8, but with a lower folded IR = 0.15 m and OR = 0.32 m. The CFRP tube arm will connect to the centerline of the 30°-gore at the 1/3rd and 2/3rd radial stations, while two smaller rods will support the free edges of the 15° side gores, as presented in Fig. 10 (b).

Shape measurements of the reflective solid surface from 3D scans of the test articles pre-and-post-deployment inside a thermal chamber will be used to assess the feasibility of this design architecture to support X-band and above radio frequencies (≥ 8 GHz) for deployable antenna reflector applications. The goal is to demonstrate with the subscale model that the novel key features of the reflector that would be used in the designs at the 10-m scale and above are effective to enable efficient stowage with minimal constraints, controlled deployment, and maintain the necessary shape accuracy in space.

V. REFERENCES

- [1] M. Toral, G. Heckler, P. Pogorelc, N. George, K. Han, "Payload performance of third generation TDRS and future services," *AIAA International Communications Satellite Systems Conference (ICSSC)*, 2017.
- [2] J. Footdale, J. Cody Griffe, M. E. Peterson, and C. Box, "Flexible composite shell design for the MARCO deployable reflector," *AIAA Scitech 2019 Forum*, 7-11 January 2019, San Diego, CA.
- [3] B. B. Allen, C. F. Willer, R. I. Harless, R. V. Valentin, R. S. Sorrell, "Compactly stowable thin continuous surface-based antenna having radial and perimeter stiffeners that deploy and maintain antenna surface in prescribed surface geometry," U.S. Patent 6,344,835 B1, Issued 5 February 2002.
- [4] P. N. Keller, M. S. Lake, D. Codell, R. Barrett, R. Taylor, M. R. Schultz, "Development of elastic memory composite stiffeners for a flexible precision reflector," *47th AIAA/ASME/ASCE/AHS Structures, Structural Dynamics, and Materials Conference*, 1-4 May 2006, Newport, RD.
- [5] R. Taylor, R. Barrett, P. Keller, D. Turse, L. Adams, "Furlable shape-memory reflector," U.S. Patent 7,710,348 B2, Issued 4 May 2010.
- [6] J. M. Fernandez, A. F. Paddock, K. Demarco, "Composite substrate reflector design," U.S. Patent Application 63/452,713 filed on March 17, 2023.
- [7] J. M. Fernandez, J. H. Kang, "Shape memory polymer composite substrate," U.S. Patent Application 63/452,712 filed on March 17, 2023.